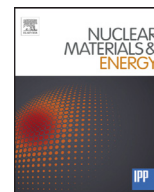




Contents lists available at ScienceDirect

Nuclear Materials and Energy

journal homepage: www.elsevier.com/locate/nme

CO₂ absorption characteristics of a blanket candidate material Li₂TiO₃ under exposure to different gas mixture

Yuichi Furuyama*, Ryoma Nakamori, Sho Nagai, Akira Taniike, Hiroaki Samata, Akira Kitamura

Graduate School of Maritime Sciences, Kobe University, Kobe 658-0022 Japan

ARTICLE INFO

Article history:

Received 14 November 2015

Accepted 15 September 2016

Available online xxx

Keywords:

CO₂ absorption
Blanket material
Li₂TiO₃
XRD
NRBS
Humidity

ABSTRACT

In order to investigate the CO₂ absorption characteristics of the low- and high-density Li₂TiO₃ samples, X-ray diffraction (XRD) and non-Rutherford backscattering spectroscopy (NRBS) analyses have been performed. Crystallographic structure of a sintered sample is decided by the XRD analysis, and the NRBS analysis has evaluated the amount of CO₂ absorption quantitatively. The amount of CO₂ absorption of the low-density Li₂TiO₃ samples is increased with increase of the humidity. We find that the humidity has effect on CO₂ absorption to the low-density Li₂TiO₃ samples. On the other hand, the high-density samples sintered at temperatures higher than 1,470 K absorb very little CO₂ under high humidity conditions.

© 2016 The Authors. Published by Elsevier Ltd.

This is an open access article under the CC BY-NC-ND license (<http://creativecommons.org/licenses/by-nc-nd/4.0/>).

1. Introduction

Solid blanket materials of a D-T nuclear fusion reactor should have a role to generate fuel tritium (T). Lithium (Li) compounds with a low chemical activity allowing easy treatment are best fitted for this purpose [1–8]. Especially, Li₂TiO₃ is recommended as the leading candidate among Li compounds, because Li₂TiO₃ has excellent chemical properties such as nonreactivity with H₂O [9] and relatively good T breeding properties among the solid blanket materials with a combination of neutron multipliers such as beryllium for increasing tritium breeding ratio. In this regard, there is an optimum density of Li₂TiO₃. If the Li₂TiO₃ density is too high, the T release rate becomes low due to a decreased permeability. On the other hand, if the density is lowered, the T production rate is decreased [10,11].

Lithium compounds such as Li₄SiO₄ and Li₂ZrO₃ are known as materials absorbing CO₂ at room temperature [12–15]. The carbon contamination of a blanket material should be minimized. It has been reported that C atoms included in a blanket material can form a tritiated hydrocarbon in a T recovery process [16,17]. Therefore, if a blanket material has carbon contamination, the T recovery efficiency would be decreased, because additional process of isotope separation would be required.

In addition, after CO₂ absorption, the surface layers of the Li compounds changes to Li₂CO₃. In the Li₂TiO₃ sample absorbing CO₂, properties necessary as a blanket material such as T release properties, and both thermal and chemical stabilities could be deteriorated, and Li density reduction might occur.

However, the CO₂ absorption properties of Li₂TiO₃ have not yet been studied. In the present paper, we point out that from the CO₂ absorption point of view there is an optimum density of Li₂TiO₃, which is consistent with the optimum determined from the T breeding point of view. In order to investigate the CO₂ absorption properties, we have exposed the Li₂TiO₃ samples with various densities to gases with various compositions; dry CO₂ gas, atmosphere, dry air and moist air. X-ray diffraction (XRD) and non-Rutherford backscattering spectroscopy (NRBS) analyses are carried out to the samples after four case exposures, and crystallographic structure of the exposed samples and the amount of CO₂ absorption are investigated [18,19].

In this work, it is shown that the amount of CO₂ absorbed by the low-density Li₂TiO₃ samples increases with increasing humidity, and that humidity of the exposure gas has a remarkable effect on the CO₂ absorption to the low-density Li₂TiO₃ samples. On the other hand, the amount of CO₂ absorption of the high-density Li₂TiO₃ samples is very little even under high humidity conditions.

2. Experimental

We have prepared the Li₂TiO₃ samples used in the present work by the solid-phase reaction method with Li₂CO₃ (99.9%,

* Corresponding author.

E-mail address: furuyama@maritime.kobe-u.ac.jp (Y. Furuyama).

<http://dx.doi.org/10.1016/j.nme.2016.09.015>

2352-1791/© 2016 The Authors. Published by Elsevier Ltd. This is an open access article under the CC BY-NC-ND license (<http://creativecommons.org/licenses/by-nc-nd/4.0/>).

Table 1
Sintering parameters and sample densities of the Li_2TiO_3 samples.

	Li_2CO_3 : TiO_2 (molar ratio)	Presintering condition		Pressurizing condition	Main sintering condition		Sample density / Theoretical density [%T.D.]
		Temperature [K]	Time [h]		Temperature [K]	Time [h]	
#1	1.0:1.0	1000	5	40 MPa 3 min	1000	5	38
#2							39
#3							40
#4							41
#5							41
#6					1200	8	75
#7							80
#8							85
#9							88
#10					1473	40	90
#11							91
#12							93
#13							94
#14					94		

Nacalai Tesque) and the TiO_2 powders (99.9%, Nilaco Co., Ltd.). The Li_2CO_3 and the TiO_2 powders were finely pulverized using an agate mortar and a pestle, and were stirred. The mixed powders were compressed and molded for 3 minutes at a pressure of 5 MPa using a press machine.

We have sintered the molded sample at temperatures from 973 K to 1500 K using an electric furnace (As one Co., Ltd.). The sintering conditions for the samples are summarized in Table 1. The low-density Li_2TiO_3 samples were made with sintering for 5 h at temperatures of 973 K – 1000 K. As theoretical mass density of Li_2TiO_3 is 3.43 g/cm³, the ratio of the sample mass density to the theoretical mass density was 0.40, which we call “40%T.D.”.

The medium- and the high-density samples were made by re-sintering the presintered low-density samples as the starting materials. After pulverizing the presintered samples again and molding them, we sintered the samples with densities of 75%T.D.–94%T.D. at temperatures from 1200 K to 1500 K for 8 – 40 h. The sintered samples were disk-shaped with thickness of 2 mm and diameter of 15 mm. We measured the sample mass with a microbalance and the volume with a vernier caliper to calculate the density.

The samples were put in a vacuum chamber evacuated to a pressure of 1 Pa, and were exposed at room temperature to dry CO_2 gas, atmosphere, dry air and moist air at 1 atm. In the case of exposure to moist air, we set a beaker filled with water in the chamber kept at high humidity (> 34,000 ppm). A digital thermohygrometer FL-02 (Tokyo Glass Kikai) was set in the vacuum chamber. The humidity during exposure to dry CO_2 gas and dry air was less than 7000 ppm, while that during exposure to atmosphere was 20,000 – 30,000 ppm.

Samples used in this work were lithium compounds of a Li_2TiO_3 . The NRBS analysis is highly sensitive to Li isotopes, and is very effective for blanket material analysis [20]. Placing the sample at the center of the target vacuum chamber, the analyses were performed using 2.6-MeV-proton beams and a silicon surface barrier

detector (SSBD) located at 165° with respect to the direction of the beam incidence.

The crystallographic structure of the prepared Li_2TiO_3 samples was investigated by XRD analysis using RINT2000 (Rigaku) with Cu-K α X-ray at room temperature. The simulation of powder XRD patterns was performed using a Rietveld-analysis program RIETAN [21] and the crystal data for Li_2TiO_3 [22], Li_2CO_3 [23], and TiO_2 [24].

3. Results and discussion

3.1. Low-density Li_2TiO_3 samples under various exposure conditions

XRD analysis was performed on the low-density Li_2TiO_3 samples (41%T.D.) after exposure to dry CO_2 gas in order to investigate crystallographic structure change of Li_2TiO_3 . The powder XRD spectra are shown in Fig. 1 in comparison with the typical as-sintered sample (39%T.D.). The vertical axis is X-ray intensity, and the horizontal axis is the diffraction angle 2θ . Simulation spectra of Li_2TiO_3 , Li_2CO_3 and TiO_2 are also shown in this figure. The powder XRD spectral pattern of the as-sintered sample is in good agreement with the simulation spectrum; peaks are observed at $2\theta = 19^\circ, 36^\circ, 44^\circ, 48^\circ, 58^\circ, 63^\circ$ and 67° , which indicates that the sintered samples are converted almost perfectly to Li_2TiO_3 . In the spectrum of the low-density Li_2TiO_3 sample after the exposure to CO_2 gas for 2000 h, the XRD peaks of Li_2CO_3 are observed at $2\theta = 21^\circ, 31^\circ$, and 32° . This clearly indicates that Li_2TiO_3 absorbs CO_2 and then forms Li_2CO_3 and TiO_2 by the dry CO_2 gas exposure.

In XRD spectra of the sample (38%T.D.) exposed to atmosphere for 2000 h, diffraction peaks at $2\theta = 19^\circ, 44^\circ, 58^\circ$ and 63° (Li_2TiO_3), peaks at $21^\circ, 31^\circ$ and 32° (Li_2CO_3) are observed similarly to the sample exposed to CO_2 . The Li_2TiO_3 sample also absorbs CO_2 under long-time exposure to atmosphere, and forms Li_2CO_3 and TiO_2 similarly to the exposure to CO_2 gas.

The ratio of the Li_2CO_3 peak intensity ($2\theta = 32^\circ$) to Li_2TiO_3 peak intensity ($2\theta = 19^\circ$), I_{32}/I_{19} , is a quantitative measure for the de-

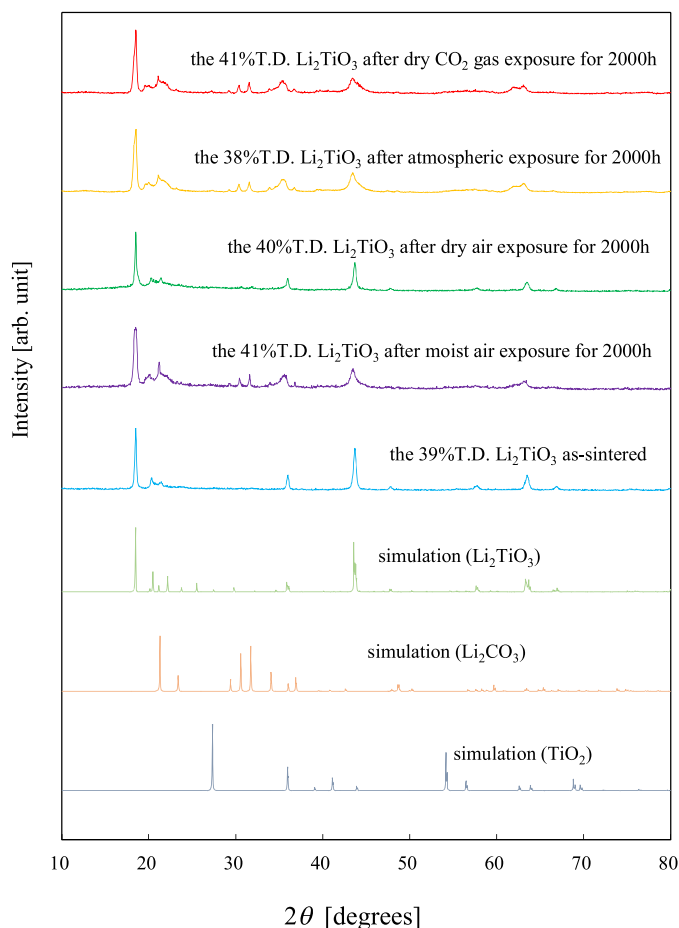


Fig. 1. XRD patterns of the as-sintered Li_2TiO_3 sample and changes of XRD patterns of the low-density sample after exposure to dry CO_2 gas, atmosphere, dry air and moist air for 2000 h.

gree of CO_2 absorption. For the atmospheric and the CO_2 gas exposure sample, the values of I_{32}/I_{19} were almost equal, that is the CO_2 absorption amount were comparable. Since the CO_2 content in atmosphere (only 0.035 vol. %) is overwhelmingly less than CO_2 in the CO_2 gas, the above result means that the atmosphere-exposed sample absorbs CO_2 very selectively.

On the other hand, in XRD spectra of the low-density sample (40%T.D.) exposed to dry air for 2000 h, the Li_2CO_3 peaks ($2\theta = 21^\circ$, 31° and 32°) are observed with much smaller amplitude in addition to the Li_2TiO_3 peaks ($2\theta = 19^\circ$ and 44°). Calculating the intensity ratio I_{32}/I_{19} , we found that the dry air exposure is clearly much less effective than that to CO_2 gas and to atmosphere. The CO_2 concentration in the dry air is essentially equal to that in the atmosphere. But the amount of Li_2CO_3 produced under dry air exposure is much less than that under atmosphere. In the present work, the humidity of atmosphere is 20,000~30,000 ppm, while that of the dry air is less than 7000 ppm. It is concluded that the humidity (water vapor) has a decisive effect on CO_2 absorption.

The exposure to moist air (> 34,000 ppm) was also performed on the sample (41%T.D.). After 2000 h exposure, the XRD showed spectra similar to those for samples exposed to CO_2 gas and atmosphere. The intensity ratio I_{32}/I_{19} for the sample with moist air exposure is larger than those under CO_2 gas and atmosphere.

In order to measure the CO_2 absorption amount more quantitatively, the NRBS analysis for the samples before and after the exposure was performed. As a typical example, Fig. 2a shows the NRBS spectrum of the sample (41%T.D.) after moist air exposure for 2000 h compared with that of the sample before exposure. In this

figure, the scattered particle yield is plotted as a function of energy. The energies of the scattered particles depend on the target particle mass and the depth at which the target particle is located. As a result, particles scattered by atoms of a specified species form a step-function-like distribution below an energy determined by the mass of the specified atom existing on the surface, which we call "the edge energy". The edge energy of Ti, O, C and Li is about 2.4, 2.0, 1.8, 1.4 MeV, respectively. After moist air exposure, a carbon plateau came to appear, and the yield of oxygen increased as compared with the spectrum before exposure. This feature of the NRBS spectrum is common to all other samples after exposure to the CO_2 gas, atmosphere and dry air.

Fig. 2b shows depth distribution of Li, C, O and Ti deduced from the energy spectra. The reason for the apparent non-zero densities in the negative depth region and the finite width of the up edges at the surface is a finite energy resolution of the detection system. The spectra are not corrected for the energy resolution. Anyway, integrating the density over the depth from $-0.2 - 2.0 \mu\text{m}$, we obtain the areal densities of Li, C, O and Ti near the surface layers ($\sim 2.0 \mu\text{m}$) is as $N_{\text{Li}} = 4.3 \times 10^{18} \text{ cm}^{-2}$, $N_{\text{C}} = 1.4 \times 10^{18} \text{ cm}^{-2}$, $N_{\text{O}} = 9.8 \times 10^{18} \text{ cm}^{-2}$ and $N_{\text{Ti}} = 2.2 \times 10^{18} \text{ cm}^{-2}$, respectively. The composition ratio of Li:Ti:O:C is then 2.0:1.0:4.5:0.6. This ratio corresponds to the composition ratio of $\text{Li}_2\text{TiO}_3 + (0.6) \text{CO}_2$.

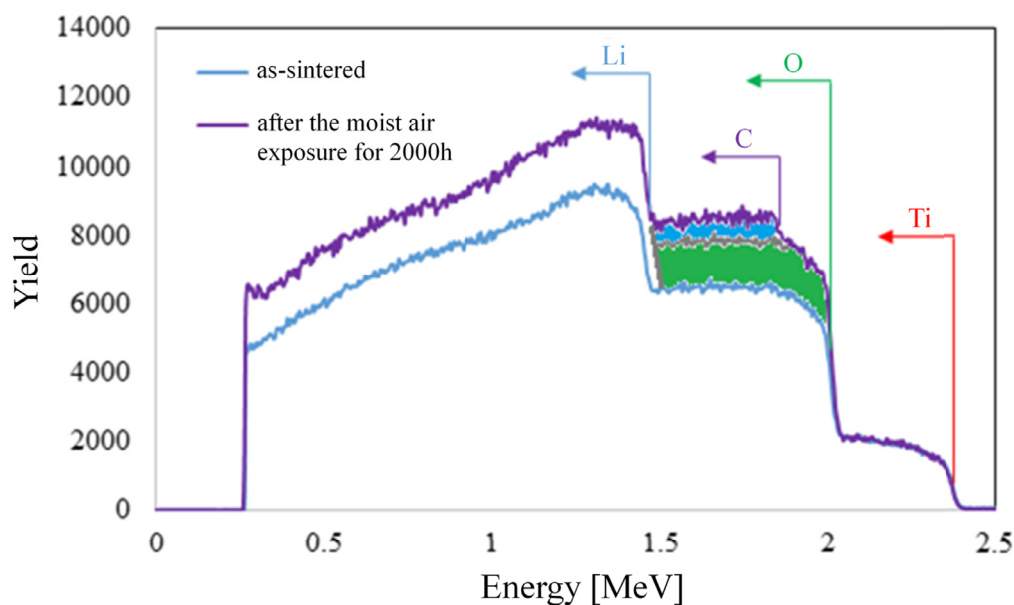
Fig. 3 shows the dependence of CO_2 absorption amount of the sample exposed to four different gases containing CO_2 as described above. We have performed the NRBS analysis for every 200 h exposure up to 2000 h, and calculated the C areal density N_{C} in each of the exposure time. The C areal density increases almost linearly in the low exposure range up to about 800 h, beyond which it approaches a saturation value depending on the exposure condition. The saturation values of N_{C} for exposure under dry CO_2 gas, atmosphere, dry air and moist air are $1.0 \times 10^{18} \text{ cm}^{-2}$, $1.0 \times 10^{18} \text{ cm}^{-2}$, $6.0 \times 10^{17} \text{ cm}^{-2}$ and $1.35 \times 10^{18} \text{ cm}^{-2}$ respectively. Under CO_2 gas, atmospheric or dry air exposure, the saturation value of the C areal density N_{C} is 1/2–3/4 of that under moist air exposure. Then, the CO_2 absorption rate dN_{C}/dt and the saturation value N_{C} of the sample under CO_2 gas exposure are both equivalent to those under atmospheric exposure. The C areal density N_{C} at saturation was $1.0 \times 10^{18} \text{ cm}^{-2}$. Comparing this value with the Ti areal density, we find that 0.5 mol of CO_2 is absorbed in 1 mol of Li_2TiO_3 in the surface region ($\sim 2 \mu\text{m}$).

Under moist air exposure, N_{C} at saturation has the maximum. The CO_2 gas and the atmospheric exposure are less effective for the CO_2 uptake. The dry air exposure is further inefficient in this regard. It can be concluded that the amount of CO_2 absorption depends more on the water vapor content than on the CO_2 content itself [25].

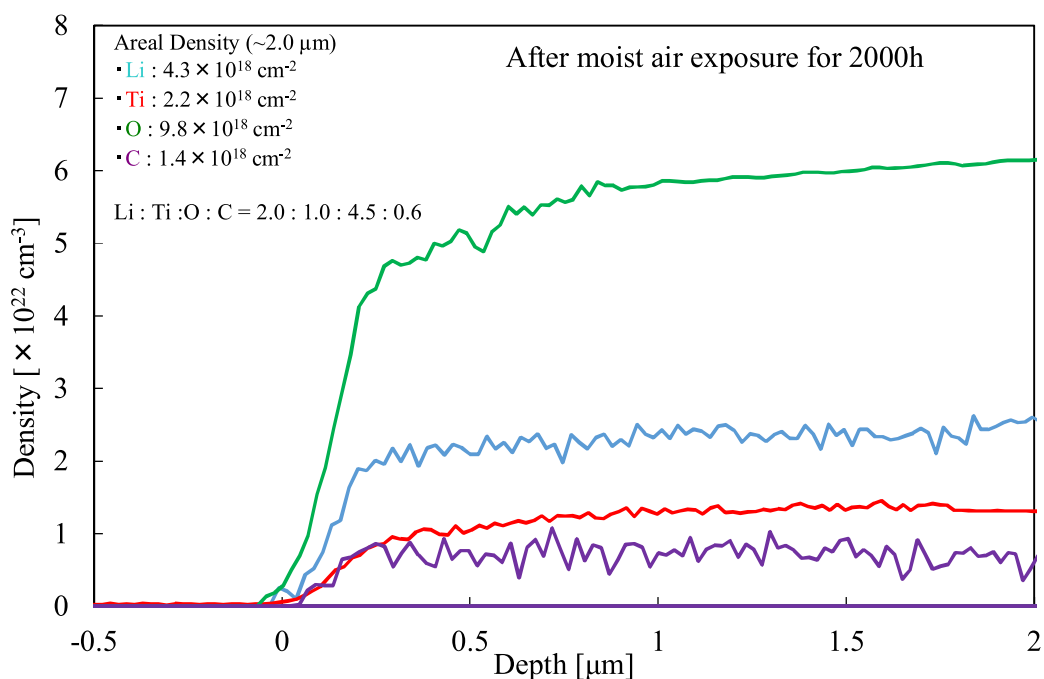
Elastic recoil detection analysis (ERDA) was performed to measure hydrogen distributions in the Li_2TiO_3 samples after CO_2 exposure and standard Li_2CO_3 samples. However, change of H concentration in the Li_2TiO_3 and Li_2CO_3 samples was not observed near the surface layers. The water molecules H_2O adsorbed/absorbed on the sample surface might have a function to attract Li ions and promote the CO_2 absorption on the sample surface. The mechanism of the CO_2 uptake is yet to be identified.

3.2. High-density Li_2TiO_3 samples under various exposure conditions

We have performed powder XRD analysis for the high-density Li_2TiO_3 sample (approximately 90%T.D.) after atmospheric, dry air and moist air exposures in order to investigate changes of crystalline structure after exposure. Fig. 4 shows XRD spectra for the high-density samples (88 - 93%T.D.) exposed to atmosphere, dry air and moist air. The exposure time was 2000 h. This figure also shows simulation spectra of Li_2TiO_3 , Li_2CO_3 and TiO_2 , and spectra of the as-sintered high-density sample.



a



b

Fig. 2. (a) The NRBS spectra measured with a 2.6-MeV proton beam for the low-density Li_2TiO_3 sample (41%T.D.) after exposure to moist air for 2000 h. The NRBS spectra of the as-sintered Li_2TiO_3 sample are also shown for comparison. (b) Depth distribution of Li, C, O and Ti in the low-density Li_2TiO_3 sample (41%T.D.) exposed to moist air for 2000 h.

All high-density samples after exposure have Li_2TiO_3 peaks at $2\theta = 19^\circ, 44^\circ, 58^\circ$ and 63° . On the other hand, the Li_2CO_3 peaks were not observed. This means that high-density samples (88 - 93%T.D.) did not change their composition after atmospheric and dry air exposures for 2000 h. This is true also for the high-density sample after moist air exposure under which the low-density sample is most likely to absorb CO_2 .

The FWHM of Li_2TiO_3 peaks at $2\theta = 19^\circ, 44^\circ$ and 58° of the high-density Li_2TiO_3 XRD spectra is smaller than that of the low-

density sample. This means that the grain size of Li_2TiO_3 is large and the high-density samples sintered at high temperature include many large grains. In other words, vacancies and grain boundaries in the sample are decreased, and the sample density is increased.

The samples (88 - 94%T.D.) after exposure to CO_2 , atmosphere, dry and moist air, we did the NRBS analysis for every 200 h up to 2000 h. Values of C areal density N_C under four exposure conditions of the high-density samples were plotted in Fig. 3. The NRBS spectra are similar to those of the as-sintered sample with no C

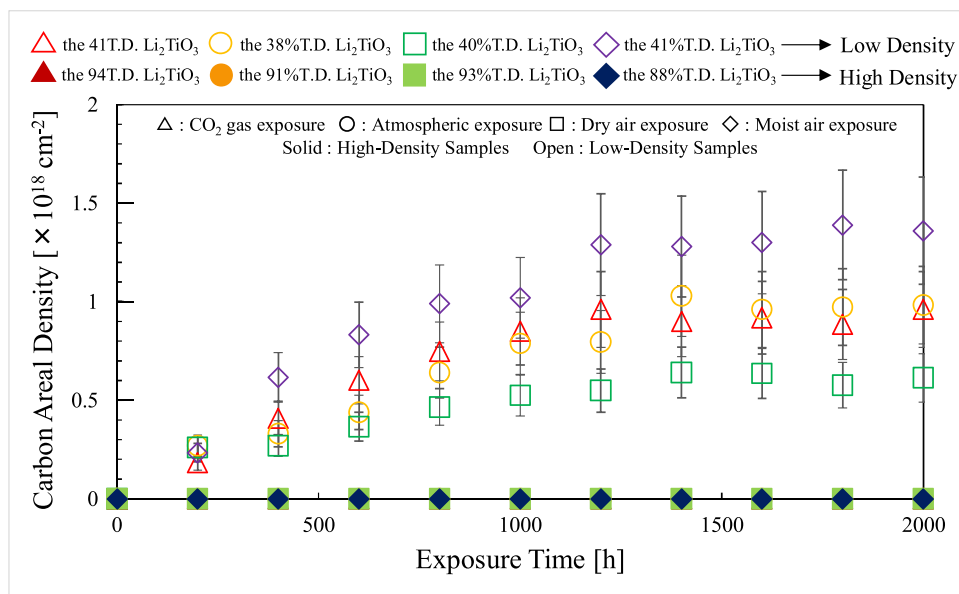


Fig. 3. Dependence of the C areal density on time of exposure to dry CO₂ gas, atmosphere, dry air and moist air to the low- and high-density samples.

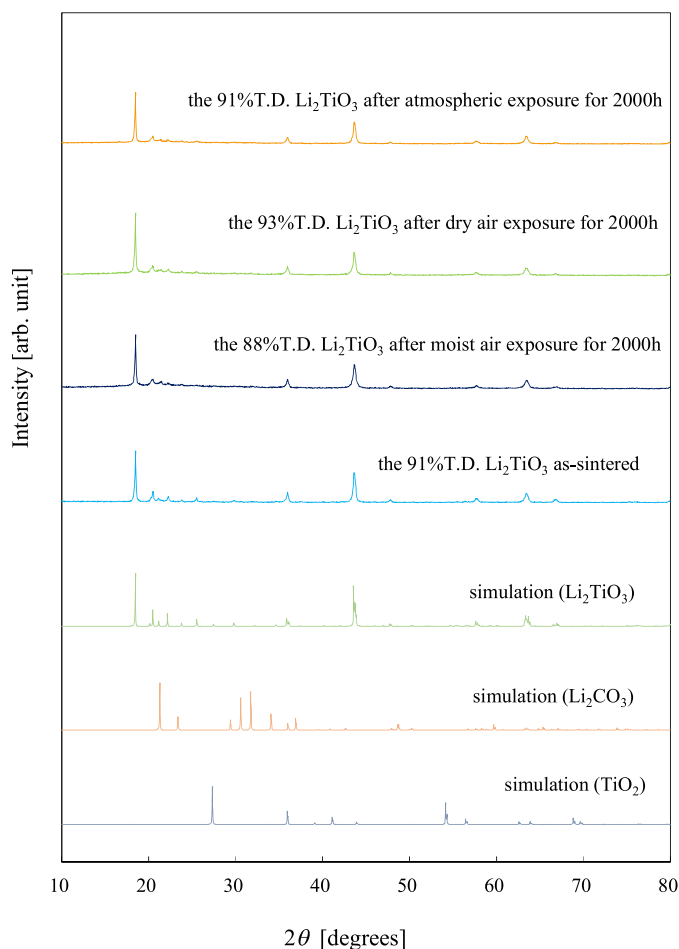


Fig. 4. XRD patterns of the as-sintered Li₂TiO₃ sample and changes of XRD patterns after exposure to atmosphere, dry air and moist air for 2000 h in the high-density sample.

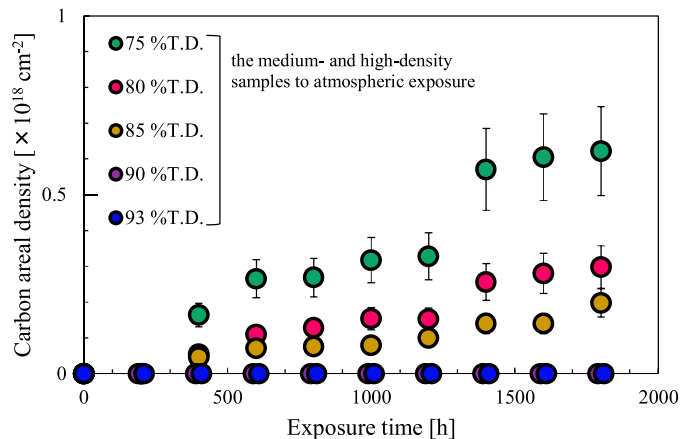


Fig. 5. Dependence of C areal density on the atmospheric exposure time for the samples with various densities.

peaks / plateau. This agrees with the XRD results. We make the high-density sample, CO₂ absorption might be suppressed. It can be concluded therefore that we have to make the Li₂TiO₃ sample density as high as possible to minimize CO₂ absorption and associated composition change.

In order to find a threshold density for CO₂ absorption, we performed atmospheric exposure to the medium-density (75 - 85%T.D.) and the high-density (90, 93%T.D.) samples to compare the amount of CO₂ absorption. Fig. 5 shows growth of the C areal density with atmospheric exposure time.

In this figure, the C areal density N_C is plotted as function of exposure time. Focusing our attention on three samples (75, 80, 85%T.D.), we find that N_C increases with increasing exposure time and decreasing density consistently with Fig. 5. On the other hand, the two samples (90, 93%T.D.) absorb almost no CO₂. Therefore, we can conclude that the threshold sample density is about 90%T.D.

As for the sintering condition (See Table 1), samples with density greater than about 90%T.D. requires the sintering temperature of 1473 K or higher. In Kleykamp report [26], at the range of room temperature to 1428 K, the crystalline structure of Li₂TiO₃ is monoclinic, and changes to cubic crystal at 1428 K or higher. But in the

present sample preparation, once we sintered at 1473 K or higher, we cooled the sample by natural heat release. Actually, XRD spectra indicate that the high-density Li_2TiO_3 samples are very similar to the simulation spectra of monoclinic Li_2TiO_3 , and not to those of cubic one.

The exposures to the ground powder samples sintered at 973 K for 5 h and then at 1473 K for 40 h, and the ground powder sample sintered only at 973 K for 5 h (presintered) were performed. We compared the NRBS spectra of the former sample with those of the latter sample after atmospheric exposure for 400 h. No C peaks / plateau were observed in the NRBS spectra of the former sample. On the other hand, a C plateau and increase in the yield of O were observed in the NRBS spectra of the latter sample. According to the result of our past experiments [ref.], a powder Li_2TiO_3 sample absorbs more CO_2 than a molded sample, and the CO_2 absorption rate is also high. From the results, Li_2TiO_3 sintered at 1473 K or higher absorbs almost no CO_2 , even if it is ground to micronize to powder Li_2TiO_3 .

Accordingly, the CO_2 absorption property of Li_2TiO_3 largely depends on sample preparing condition, and can be greatly suppressed by sintering at temperatures higher than 1470 K. As mentioned above, while the samples sintered at 1473 K and cooled by natural heat release does not have cubic crystal, the FWHM of the Li_2TiO_3 peaks in XRD becomes smaller unlike those sintered at low temperature. This tells us that the grains grow, and the sample changes to have highly crystalline structure. The reason why the high-density sample absorb little CO_2 can be considered to be the highly crystalline structure grown by sintering at temperatures higher than 1470 K making the sample more dense, which reduces the effective surface area of sample reacting with CO_2 .

4. Conclusions

The exposures of the low-density Li_2TiO_3 samples for 2000 h to dry CO_2 gas (H_2O content is less than 7000 ppm), atmosphere (20,000–30,000 ppm), dry air (less than 7000 ppm) and moist air (more than 34,000 ppm) have been performed. The XRD analysis shows that the low-density Li_2TiO_3 samples under four different exposure conditions have absorbed CO_2 , and the composition of a part of the Li_2TiO_3 samples has changed to a mixture of Li_2CO_3 and TiO_2 . The NRBS analysis of the samples shows that C areal density absorbed as CO_2 by exposures is increased with exposure time. The amount of absorbed CO_2 is saturated at exposure time of about 1200 h. The saturated value decreases with decreasing humidity; i.e., in order of moist air, atmosphere, dry CO_2 gas and dry

air. We have found that Li_2TiO_3 do not react with H_2O , however the humidity is the most important factor affecting the amount of absorbed CO_2 . Since the low-density Li_2TiO_3 samples have many vacancies and micro-pores with the small grain size, as the XRD analysis shows for the low-density sample, the effective surface area will be large, and therefore the amount of CO_2 absorption is increased. In addition, it is inferred that H_2O absorbed on the sample surface might have a function to attract Li ions and promote the CO_2 absorption on the sample surface.

On the other hand, Li_2CO_3 peaks in the XRD spectra are not observed in any case of the high-density sample exposed for long time. The low-density sample most absorbed CO_2 under moist air exposure, whereas no C peaks / plateau are observed in the NRBS spectra of the high-density sample after moist air exposure for 2000 h. In the case of Li_2TiO_3 sintered at high temperatures (higher than 1470 K), as observed with the XRD analysis for the high-density sample, grains grow, and the sample becomes to have highly dense structure, which makes CO_2 absorption hard to occur. The situation is similar for other powder samples sintered at high temperatures. This result indicates that a sample with 85%T.D. could be the most suitable one for the blanket materials absorbing little amount of CO_2 and breeding reasonable amount of T.

References

- [1] D.L. Smith, *J. Nucl. Mater.* 103–104 (1981) 19–30.
- [2] C.E. Johnson, G.W. Hollenberg, *J. Nucl. Mater.* 122–123 (1984) 871–881.
- [3] M. Dalle Donne, et al., *J. Nucl. Mater.* 212–215 (1994) 69–79.
- [4] J.P. Kopasz, J.M. Miller, C.E. Johnson, *J. Nucl. Mater.* 212–215 (1994) 927–931.
- [5] R.F. Mattas, M.C. Billone, *J. Nucl. Mater.* 233–237 (1996) 72–81.
- [6] A.R. Raffray, et al., *J. Nucl. Mater.* 307–311 (2001) 21–30.
- [7] H. Kawamura, et al., *Nucl. Fusion* 43 (2003) 675–680.
- [8] K. Tsuchiya, et al., *Nucl. Fusion* 47 (2007) 1300–1306.
- [9] N. Roux, et al., *J. Nucl. Mater.* 233–237 (1996) 1431–1435.
- [10] J.M. Miller, et al., *J. Nucl. Mater.* 212–215 (1994) 877–880.
- [11] N. Roux, et al., *Fusion Eng. Des.* 27 (1995) 154–166.
- [12] M. Kato, et al., *Int. J. Appl. Ceram. Technol.* 2 (6) (2005) 467–475.
- [13] M.J. Venegas, et al., *Ind. Eng. Chem. Res.* 6 (2007) 2407–2412.
- [14] L. Guo, X. Wang, C. Zhong, L. Li, *Appl. Surf. Sci.* 257 (2011) 8106–8109.
- [15] S. Ueda, et al., *ISIJ Int.* 51 (4) (2011) 530–537.
- [16] S. Nasu, et al., *J. Nucl. Mater.* 68 (1977) 261–264.
- [17] H. Kudo, et al., *J. Inorg. Nucl. Chem.* 40 (1978) 363–367.
- [18] Y. Furuyama, et al., *J. Nucl. Mater.* 442 (2013) S442–S446.
- [19] Y. Furuyama, et al., *J. Nucl. Mater.* 455 (2014) 527–530.
- [20] Y. Furuyama, et al., *Nucl. Instrum. Methods Phys. Res. B.* 331 (2014) 96–101.
- [21] F. Izumi, T. Ikeda, *Mater. Sci. Forum* 321–324 (2000) 198–205.
- [22] J.F. Dorrian, R.E. Newnham, *Mater. Res. Bull.* 4 (1969) 179–184.
- [23] J. Zemann, *Acta Crystallogr.* 10 (1957) 664–666.
- [24] W.H. Baur, *Acta Crystallogr.* 9 (1956) 515–520.
- [25] K. Essaki, et al., *J. Chem. Eng. Jpn.* 37 (6) (2004) 772–777.
- [26] H. Kleykamp, *Fusion Eng. Des.* 61–62 (2002) 361–366.